

Band lineup between silicon and transparent conducting oxides

B. Höffling,^{a)} A. Schleife, F. Fuchs, C. Rödl, and F. Bechstedt

*Institut für Festkörperteorie und -optik, European Theoretical Spectroscopy Facility (ETSF),
Friedrich-Schiller-Universität, Max-Wien-Platz 1, 07743 Jena, Germany*

(Received 3 June 2010; accepted 22 June 2010; published online 23 July 2010)

Modern quasiparticle calculations based on hybrid functionals are used to predict natural band discontinuities between silicon and In_2O_3 , ZnO , and SnO_2 by two alignment methods, a modified Tersoff method for the branch-point energy and the Shockley–Anderson model via the electron affinity rule. The results of both methods are found to be in good agreement. A tendency for misaligned type-II heterostructures is predicted, indicating efficient electron-hole separation at the Si-oxide interfaces. © 2010 American Institute of Physics. [doi:10.1063/1.3464562]

Transparent conducting oxides (TCOs) such as In_2O_3 , SnO_2 , and ZnO are frequently applied as transparent electrodes in optoelectronic or photovoltaic devices and sensors.¹ They are widely used in Si photonics and Si-based solar cells.² Therefore, knowledge about the interfaces of TCOs and crystalline Si layers is extremely important. This holds especially for the energy band alignment at their heterostructures.^{3,4} However, band discontinuities and accompanying band lineups are virtually unknown for Si/TCO heterostructures. Parameters such as the ionization energy I , the electron affinity A , and the branch point energy E_{BP} are controversially discussed in the literature.^{5–10} The surface electron accumulation or surface electron depletion are also under debate.¹¹

The Si-TCO interfaces exhibit an enormous complexity since the two materials in contact are mismatched with respect to the crystal structure, the lattice constants, and the atomic valencies. As a consequence, difficulties to investigate and interpret Si-oxide heterojunctions arise from the large variety of different surface orientations and interface geometries. One possibility to avoid these problems is the application of theoretical methods which do not account for the details of the atomic geometry of the interfaces but make use of appropriate more macroscopic models of aligning electronic structures. They are based on modern quasiparticle (QP) band-structure theory¹² to compute characteristic energies and band discontinuities,⁹ which has recently been shown to yield accurate description of TCOs.^{13,14} In this letter, the resulting band structures are used to compute the ionization energies, electron affinities, and branch-point energies for Si, In_2O_3 , SnO_2 , and ZnO , which in turn are then used to align the electronic bands at both sides of the interface and to derive band discontinuities.

The fundamental parameters determining the electronic properties of heterostructures are the relative positions of the conduction band minimum (CBM) E_c and the valence band maximum (VBM) E_v at the interface. For pseudomorphic interfaces there exists a well defined procedure to compute the band discontinuities ΔE_v and ΔE_c at the interface applying *ab initio* electronic-structure calculations.¹⁵ However, for heterovalent, heterostructural, and heterobonded interfaces theoretical and experimental data are at variance. Since reliable models do not exist, we determine the band offsets by

methods which require no knowledge of the structural details of the interfaces. The conduction- and valence-band discontinuities ΔE_c and ΔE_v between the oxides and crystalline silicon are calculated using two different band alignment methods employing the branch-point energies or the vacuum levels. In the case of In_2O_3 we study the rhombohedral (rh) and the body centered cubic (bcc) bixbyite geometries. ZnO crystallizes in wurtzite (wz) structure while for SnO_2 the most important rutile (rt) geometry is investigated. The atomic geometries of the oxides and silicon are computed in the framework of density functional theory (DFT) using the local density approximation (LDA) for exchange and correlation (XC). All computations are performed with the Vienna *ab initio* simulation package.¹⁶ The electronic wave functions are expanded using plane waves up to kinetic energies of 450 eV, 550 eV, 450 eV, and 500 eV for Si, In_2O_3 , SnO_2 , and ZnO , respectively. The projector-augmented wave method is used to model the electron-ion interaction. The resulting lattice constants are $a_0=5.402$ Å for Si, $a_0=10.09$ Å for bcc- In_2O_3 , $a=5.48$ Å and $c/a=2.63$ for rh- In_2O_3 , $a=4.74$ Å and $c/a=0.68$ for rt- SnO_2 , and $a=3.28$ Å and $c/a=1.61$ for wz- ZnO .

The branch point energy alignment requires solely the QP band structures of the bulk materials. They are determined by iterating the QP equation.¹² In the zeroth step the XC self-energy is approximated by the spatially nonlocal XC potential of Heyd, Scuseria, and Ernzerhof (HSE03).¹⁷ In the next step the QP band structures are determined using perturbation theory. The QP wave functions remain unchanged and the QP shifts are computed within the G_0W_0 approach. The relative positions of E_c and E_v define the fundamental energy gap E_g . The calculated gaps for Si and the TCOs are listed in Table I. The results are close to measured values.^{18–20} The branch point energy E_{BP} is calculated by a modification of the Tersoff method²¹ as the mean value of the Brillouin zone averages of the topmost valence bands and the lowest conduction bands (see Ref. 9 for details). The bulk band structures used to compute E_{BP} have a strong relationship to surface states, so-called virtual gap states.²² The charge neutrality level is identified as the level at which the surface states change from donor- to acceptor-like behavior. Therefore the surface Fermi level is pinned at this energy level, which can be exploited for band alignment. Then the branch-point energies E_{BP} and fundamental gaps E_g lead to the natural band discontinuities

^{a)}Electronic mail: benjamin.hoeffling@uni-jena.de.

TABLE I. Fundamental gaps E_g , branch point energies E_{BP} , electron affinities A , and ionization energies I of TCO and Si. All values in eV. The surface orientation used for the calculation of I and A is given by a cubic axis or the c -axis for rh and wz. For rt a direction perpendicular to the c -axis is chosen. Experimental values are given in parentheses.

Crystal	E_g	E_{BP}	A	I
rh-In ₂ O ₃	3.31 (3.02) ^a	3.79 (3.50) ^a	6.11	9.41
bcc-In ₂ O ₃	3.15 (2.93) ^a	3.50 (3.58) ^a	5.95 (4.1–5.0) ^f	9.10 (7.7–8.6) ^f
wz-ZnO	3.21 (3.38) ^b	3.40 (3.2, 3.78) ^{d,e}	5.07 (4.25–4.95) ^g	8.24 (7.82, 8.35) ^{g,h}
rt-SnO ₂	3.64 (3.6) ^c	3.82	4.10 (4.44) ⁱ	7.73 (8.04) ⁱ
Si	1.29 (1.17) ^b	0.29	4.54 (4.0–4.2) ^h	5.83 (5.15–5.33) ^h

^aReferences 11 and 18.

^bReference 19.

^cReference 20.

^dReference 6.

^eReferences 24 and 28.

^fReference 5.

^gReferences 26 and 28.

^hReference 22.

ⁱReference 7 and 28.

$$\Delta E_c = [E_g(\text{oxide}) - E_{BP}(\text{oxide})] - [E_g(\text{Si}) - E_{BP}(\text{Si})],$$

$$\Delta E_v = E_{BP}(\text{oxide}) - E_{BP}(\text{Si}), \quad (1)$$

as the relative positions of the band extrema E_v and E_c at both sides of the interface.²³

The vacuum level alignment method takes an intermediate step by studying surfaces or vacuum-oxide interfaces first. The surface properties of the oxides are computed in the framework of DFT-LDA. For each heterostructure the surface barrier is modeled by a material slab with normal direction z , followed by a thick vacuum layer. The electrostatic potential acting on the ions is derived from the effective single-particle potential occurring in the Kohn–Sham equation. The plane-averaged potential $\bar{V}(z)$ is then compared with that of the QP bulk calculations. For an unreconstructed surface of a given orientation this allows the determination of the absolute positions of the band edges E_v and E_c in QP approximation with respect to the vacuum level E_{vac} . The energy differences $I = E_{vac} - E_v$ and $A = E_{vac} - E_c$ define the ionization energy I and the electron affinity A for such an idealized surface. The two quantities are directly related to the fundamental QP gap by $E_g = I - A = E_c - E_v$. The calculated I and A are used to derive natural band discontinuities in the framework of the electron affinity rule or, more general, the Shockley–Anderson model by

$$\Delta E_c = A(\text{Si}) - A(\text{oxide}),$$

$$\Delta E_v = I(\text{oxide}) - I(\text{Si}). \quad (2)$$

Here the band alignment is made using the vacuum level E_{vac} . The Shockley–Anderson model completely disregards the existence of interface states and assumes a vanishing density of interface states.

The band edges and electrostatic potentials as calculated by the vacuum level alignment method are presented in Fig. 1(a). They clearly show that in a certain distance from the

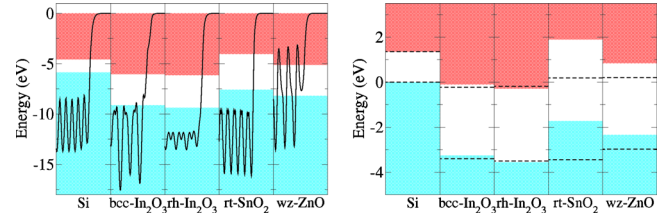


FIG. 1. (Color online) (a) Planar-average electrostatic potential $\bar{V}(z)$ near a surface (solid line) for Si(001), bcc-In₂O₃(001), rh-In₂O₃(0001), rt-SnO₂(01 $\bar{1}$ 0), and wz-ZnO(0001). The related QP conduction and valence bands are indicated by shading. The vacuum level is used as energy zero. (b) Conduction-band E_c and valence-band E_v edges for silicon, bcc-In₂O₃, rh-In₂O₃, rt-SnO₂, and wz-ZnO. The shaded areas indicate the band lineup via the vacuum level E_{vac} , the dashed horizontal lines show the valence and conduction bands using alignment via the branch-point energy E_{BP} . The silicon VBM is used as energy zero.

surface the electrostatic potentials exhibit a bulklike behavior. Within the surface region there is a steep increase to a plateau which represents the vacuum level E_{vac} . Therefore, the distances between this plateau and the energy levels E_v and E_c obtained from their relative position to the bulk potentials yield the ionization energies and electron affinities listed also in Table I. The measurements of surface accumulation for undoped In₂O₃ and doped samples indicate values $E_{BP} = 3.5\text{--}3.6$ eV (Refs. 11 and 18) in excellent agreement with the QP predictions. For wz-ZnO,⁶ recent measurements indicate a value of $E_{BP} = 3.78$ eV.²⁴ Another study gives values of $E_{BP} = 3.52\text{--}3.71$ eV.²⁵ Because of a similar strong dispersion of the lowest conduction band as in In₂O₃ and ZnO, the branch point of SnO₂ also lies above the CBM. Experimental data is not available for SnO₂. The positions of calculated hydrogen-induced defect levels in the oxides also indicate a Fermi stabilization above the CBM for ZnO.^{7,23}

The surface properties of In₂O₃ and of Sn-doped-In₂O₃ (Indium-Tin Oxide, ITO) are poorly known. In dependence on the doping concentration the electron affinity seems to vary in the range $A = 4.1\text{--}5.0$ eV (see Ref. 5 and references therein). Together with a previously adapted gap of 3.6 eV, ionization energies of $I = 7.7\text{--}8.6$ eV may be derived. Our theoretical values seem to overestimate the experimental findings slightly. The discrepancies to the largest experimental values are of the order of 0.5 eV. One reason could be the neglect of vertex corrections in the XC self-energy. Apart from uncertainties in the theoretical description several problems of the real-structure surfaces such as doping influence, coverage (and hence surface dipole), and sample quality have to be mentioned. Also the gap value 3.6 eV taken from optical measurements deviates by 0.5 eV from the recently predicted one.¹⁸

In the case of wz-ZnO there is a wide range of measured values. In their original work Jacobi *et al.*²⁶ found electron affinities up to $A = 4.5$ and 4.6 eV in dependence of surface orientation and termination. Another electrically measured electron affinity amounts to $A = 4.64$ eV.²⁷ Values $A = 4.25$ eV and $A = 4.95$ eV have been derived in dependence on the surface polarity.²⁸ With a gap of 3.4 eV (Ref. 7) a maximum value $I = 8.35$ eV results. A measurement gave $I = 7.82$ eV.²² The knowledge of the surface properties of SnO₂ is poorer. Measurements gave $A = 4.44$ eV (Ref. 28) and in combination with a gap $E_g = 3.6$ eV an ionization energy $I = 8.04$ eV.⁷ The ionization energy for Si is rather fixed in the interval $I = 5.15\text{--}5.33$ eV for different orientations and

TABLE II. Band discontinuities ΔE_c and ΔE_v Eqs. (1) and (2) of oxides with respect to the band positions of silicon derived by two different alignment methods in comparison to experimental data. All values in eV.

Si heterointerface with	Via E_{BP}		Via I and A		Experiment	
	ΔE_c	ΔE_v	ΔE_c	ΔE_v	ΔE_c	ΔE_v
rh-In ₂ O ₃	-1.48	3.50	-1.57	3.58
bcc-In ₂ O ₃	-1.35	3.23	-1.42	3.27	-0.61 ^a	2.6 ^a
wz-ZnO	-1.17	3.09	-0.53	2.34	-0.4 ^b	2.55 ^b
rt-SnO ₂	-1.19	3.53	0.44	1.83

^aReference 29.

^bReference 30.

reconstructions.²² These values lead to $A=4.0-4.2$ eV taking into account the Si gap of 1.17 eV. The QP values may overestimate I and A by about 0.3 eV.

The calculated band discontinuities ΔE_v and ΔE_c of the VBM and CBM, respectively, between the Si and oxide sides are listed in Table II and give rise to the band lineups as presented in Fig. 1(b). Using the branch point as universal energy level of reference to align the energy bands of Si and the TCO, we observe $\Delta E_c < 0$ and $\Delta E_v > 0$, indicating staggered type-II heterojunctions. In the case of Si-In₂O₃ we find $|\Delta E_c| > E_g(\text{Si})$. Therefore, these interface structures even represent a misaligned type-III heterostructure sometimes also called broken-gap heterostructure. For all the oxides the absolute positions of the band edges E_c and E_v using E_{BP} alignment are rather similar in Fig. 1(b). This may be interpreted as a consequence of nearly identical gaps and the validity of the common anion rule.²² In the case of the band alignment using the vacuum level, the band lineups are qualitatively conserved [cf. Fig. 1(b)]. The only significant change happens for the heterojunction Si-SnO₂. In contrast to the E_{BP} alignment the E_{vac} alignment tends more to a type-I heterostructure. This discrepancy may be attributed to the neglect of electrostatic effects occurring at surfaces and interfaces in the Tersoff method. Since a real interface would inevitably possess an interface dipole it is clear that the band discontinuities of Si-TCO heterostructures strongly depend on the surface orientations and the interface structure.¹⁰ For the remaining Si-TCO heterojunctions the band alignment via the two methods is in good agreement, indicating that both theoretical methods are useful tools for the prediction of natural band offsets, requiring no detailed knowledge of the atomic structure and stoichiometry of the interface.

Experimental values for the band discontinuities are rather rare. In the case of the Si-In₂O₃ heterojunction a barrier $\Delta E_c = -0.61$ eV for electrons going from In₂O₃ to Si has been measured by means of photoinjection.²⁹ Together with the bulk gaps $E_g = 3.1$ eV (In₂O₃) and $E_g = 1.1$ eV (Si) a valence band discontinuity of $\Delta E_v = 2.6$ eV is derived. Both the type of the heterostructure (i.e., the signs of ΔE_c and ΔE_v) and the order of magnitude are in agreement with our predictions using two different band alignment methods (cf. Table II). Band offsets $\Delta E_c = -0.4$ eV and $\Delta E_v = 2.55$ eV

have been estimated from measured electron affinity/work function values of p-Si and n-ZnO.³⁰ Both results confirm the theoretical prediction (apart from the application of the electron affinity rule for SnO₂) of a misaligned type-II heterocharacter of the Si-TCO interfaces which indicates an efficient electric separation of electron-hole pairs generated at the Si side of a solar cell structure. Only the use of SnO₂ should be restricted to ITO alloys.

The authors are grateful to T. D. Veal and P. D. C. King for valuable discussions. We acknowledge financial support from the German Federal Government (BMBF Project No. 13N9669), the Carl-Zeiss-Stiftung, the Deutsche Forschungsgemeinschaft (Project No. Be1346/20-1), and the European Community in the framework of ETSF (Grant No. 211956). Further, we thank the LRZ Munich and HLR Stuttgart for CPU time.

¹S. Lany and A. Zunger, *Phys. Rev. Lett.* **98**, 045501 (2007).

²R. W. Miles, G. Zoppi, and I. Forbes, *Mater. Today* **10**, 20 (2007).

³X. Zhang, Q. Zhang, and F. Lu, *Semicond. Sci. Technol.* **22**, 900 (2007).

⁴Z.-X. Fu, B.-X. Lin, and G.-H. Liao, *Chin. Phys. Lett.* **16**, 753 (1999).

⁵A. Klein, *Appl. Phys. Lett.* **77**, 2009 (2000).

⁶W. Walukiewicz, *Physica B* **302-303**, 123 (2001).

⁷C. Kılıç and A. Zunger, *Appl. Phys. Lett.* **81**, 73 (2002).

⁸S. P. Harvey, T. O. Mason, Y. Gassenbauer, R. Schafranek, and A. Klein, *J. Phys. D: Appl. Phys.* **39**, 3959 (2006).

⁹A. Schleife, F. Fuchs, C. Rödl, J. Furthmüller, and F. Bechstedt, *Appl. Phys. Lett.* **94**, 012104 (2009).

¹⁰W. Mönch, *Appl. Phys. Lett.* **93**, 172118 (2008).

¹¹P. D. C. King, T. D. Veal, D. J. Payne, A. Bourlange, R. G. Egdell, and C. F. McConville, *Phys. Rev. Lett.* **101**, 116808 (2008).

¹²F. Fuchs, J. Furthmüller, F. Bechstedt, M. Shishkin, and G. Kresse, *Phys. Rev. B* **76**, 115109 (2007).

¹³F. Fuchs and F. Bechstedt, *Phys. Rev. B* **77**, 155107 (2008).

¹⁴A. Schleife, C. Rödl, F. Fuchs, J. Furthmüller, and F. Bechstedt, *Phys. Rev. B* **80**, 035112 (2009).

¹⁵C. G. Van de Walle and R. M. Martin, *Phys. Rev. B* **34**, 5621 (1986).

¹⁶G. Kresse and J. Furthmüller, *Comput. Mater. Sci.* **6**, 15 (1996).

¹⁷J. Heyd, G. E. Scuseria, and M. Ernzerhof, *J. Chem. Phys.* **118**, 8207 (2003).

¹⁸P. D. C. King, T. D. Veal, F. Fuchs, C. Y. Wang, D. J. Payne, A. Bourlange, H. Zhang, G. R. Bell, V. Cimalla, O. Ambacher, R. G. Egdell, F. Bechstedt, and C. F. McConville, *Phys. Rev. B* **79**, 205211 (2009).

¹⁹*Springer Handbook of Condensed Matter and Materials Data*, edited by W. Martienssen and H. Warlimont (Springer, Berlin, 2005).

²⁰K. Reimann and M. Steube, *Solid State Commun.* **105**, 649 (1998).

²¹J. Tersoff, *Phys. Rev. B* **30**, 4874 (1984).

²²W. Mönch, *Semiconductor Surfaces and Interfaces* (Springer, Berlin, 2001).

²³C. G. Van de Walle and J. Neugebauer, *Nature (London)* **423**, 626 (2003).

²⁴P. D. C. King, R. L. Lichti, Y. G. Celebi, J. M. Gil, R. C. Vilão, H. V. Alberto, J. Piroto Duarte, D. J. Payne, R. G. Egdell, I. McKenzie, C. F. McConville, S. F. J. Cox, and T. D. Veal, *Phys. Rev. B* **80**, 081201(R) (2009).

²⁵M. W. Allen, C. H. Swartz, T. H. Myers, T. D. Veal, C. F. McConville, and S. M. Durbin, *Phys. Rev. B* **81**, 075211 (2010).

²⁶K. Jacobi, G. Zwicker, and A. Gutmann, *Surf. Sci.* **141**, 109 (1984).

²⁷W. Göpel, L. J. Brillson, and C. F. Brucker, *J. Vac. Sci. Technol.* **17**, 894 (1980).

²⁸H. Moormann, D. Kohl, and G. Heiland, *Surf. Sci.* **80**, 261 (1979).

²⁹M. Schmidt, private communication (June 17, 2009).

³⁰I.-S. Jeong, J. H. Kim, and S. Im, *Appl. Phys. Lett.* **83**, 2946 (2003).